International Journal of Scientific Research in Engineering and Management (IJSREM)
Volume: 10 Issue: 03 | March - 2026 SJIF Rating: 8.659 ISSN: 2582-3930

Comparative Performance Analysis of MPPT Algorithms for Grid-Interconnected Photovoltaic Systems

Manisha Thakur [1], Satya Prakash Makhija[2]

[1]*M. Tech scholar, department of electrical engineering, RSR RCET, Bhilai, Chhattisgarh, India*
[2]*Associate professor, department of electrical engineering, RSR RCET, Bhilai, Chhattisgarh, India*

Abstract - Based on the outcomes of this study, a comprehensive modeling and simulation framework for a renewable-energy-based hybrid microgrid system with appropriate control strategies is presented. The solar generation unit comprises a photovoltaic (PV) array coupled with a DC–DC boost converter. The boost converter is regulated using the incremental conductance (IC) MPPT algorithm along with an auxiliary maximum power point tracking technique to ensure optimal power extraction from the PV array. An IGBT is employed as the switching device in the boost converter, operating at a switching frequency of 50 kHz. The PV system is interfaced with a 1000 V DC bus, which serves as the common coupling point of the hybrid microgrid.

The grid-side network is modeled using a 120 kV, 50 Hz AC utility source, connected through a 400 V/120 kV step-up transformer. A full-bridge inverter topology utilizing IGBT switches is implemented to convert DC power into AC power. To achieve proper synchronization with the utility grid, a phase-locked loop (PLL) control scheme is employed, ensuring that the inverter output voltage matches the grid in terms of phase, frequency, and amplitude. The system is operated under solar irradiance conditions, and simulation results demonstrate that the proposed hybrid microgrid configuration successfully achieves the desired performance objectives.

Key Words: DC–DC Boost Converter; Incremental Conductance MPPT; Photovoltaic Array Model; Three-Phase Three-Level Inverter; IGBT; Phase-Locked Loop (PLL).

1.INTRODUCTION

Photovoltaic (PV) systems have become a major contributor to renewable energy generation; however, their performance is significantly affected by variations in solar irradiance and temperature. To ensure maximum energy extraction under changing environmental conditions, Maximum Power Point Tracking (MPPT) algorithms are employed to operate the PV array at its optimal operating point.

In grid-connected PV systems, efficient MPPT control is essential for improving power transfer efficiency and maintaining grid stability. Conventional MPPT techniques such as Perturb and Observe (P&O) and Incremental Conductance (INC), along with advanced control approaches, have been widely reported to enhance tracking accuracy and dynamic response. Additionally, effective inverter control is required to regulate voltage, frequency, and power quality in compliance with grid requirements.

This work evaluates the performance of MPPT algorithms in a grid-connected PV system, focusing on power oscillations, steady-state accuracy, and dynamic response under varying irradiance conditions. The influence of grid synchronization, inverter control, and energy management on system reliability is also examined. The results confirm that optimized MPPT implementation improves the efficiency and stability of PV–grid integrated systems.

The investigated system consists of photovoltaic panels interfaced with building distribution boards through five 20 kW inverters [3]–[4]. A mathematical model of a 20 kW PV array is developed in MATLAB/Simulink [5]. Two MPPT algorithms perturb and Observe (P&O) and Incremental Conductance (IncCond) are implemented in the control of a DC–DC boost converter placed between the PV array and the inverter [6]. Simulation results are validated by comparing the output power and performance parameters with measured data under corresponding irradiance conditions.

II. MATHEMATICAL MODEL OF A PV CELL

The block diagram illustrates a typical grid-connected photovoltaic (PV) power conversion system. The PV array output is first processed by a DC–DC boost converter, which regulates the PV voltage and enables Maximum Power Point Tracking (MPPT) to extract maximum available power. The boosted DC power is then fed to a DC–AC inverter, which converts it into

synchronized AC power. Finally, the conditioned AC output is delivered to the utility grid, ensuring proper voltage, frequency, and power quality compliance.

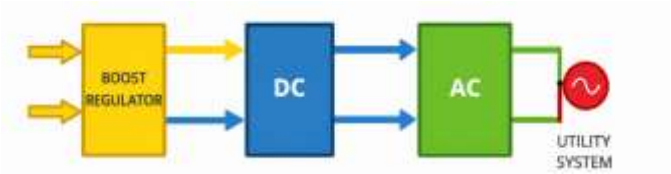

Fig 1: Block diagram of hybrid system

A photovoltaic (PV) array is a semiconductor-based energy conversion system that generates direct current (DC) electricity from solar irradiation. It consists of multiple PV modules interconnected in series and parallel configurations to achieve the required voltage and power levels. To maximize power extraction, the PV array is interfaced with a Maximum Power Point Tracking (MPPT) controller, which dynamically adjusts the operating voltage to ensure optimal DC power output. The extracted DC power is subsequently converted into alternating current (AC) by an inverter and supplied to the utility grid.

A. PV Array

An equivalent circuit of a solar cell is shown in Figure 2[1] which can be represented by (1).

$$I = I_{ph} - I_0\left[\exp\left(\frac{V+R_S I}{V_t a}\right)-1\right]-\frac{V+R_S I}{R_P} \quad (1)$$

Where:

Iph = the solar-generated current.

Io= is the diode saturation current.

Vt = NskT/q is thermal voltage of the array

Ns=number of cells connected in series

a = ideality constant of diode ;

Rs= series-resistance;

Rp= parallel-resistance.

The current generated by the sun, Iph, is linearly dependent on solar radiation and is influenced by temperature depending on the (2)[1].

$$I_{ph} = \frac{G}{G_n}\left[I_{phn} + K_i(T - T_n)\right] \quad (2)$$

where

Iph,n = Solar initiate current at the nominal-condition (25°C and 1000W/m2);

G = irradiance;

Gn = nominal irradiance;

T = cell temperature;

Tn = nominal cell temperature;

Ki =short-circuit current/temperature coefficient.

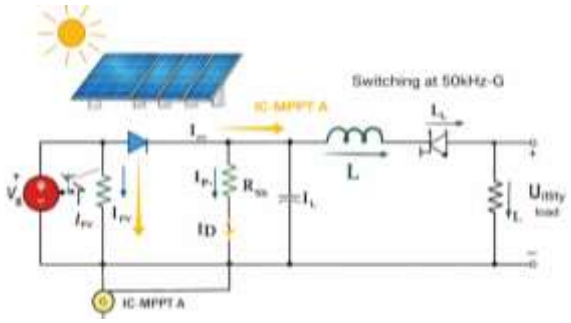

Fig 2: PV array Model

The diode impregnation current, Io which depends on temperature is given by (3)[2].

$$I = N_{pp} I_{pv} - N_{pp} I_0\left[\exp\left(\frac{V + IR_S\left(\frac{N_{ss}}{N_{pp}}\right)}{V_t a N_{ss}}\right)-1\right]-\frac{V + IR_s\left(\frac{N_{ss}}{N_{pp}}\right)}{R_p\left(\frac{N_{ss}}{N_{pp}}\right)} \quad (3)$$

Where:

Io = nominal diode saturation current.

q=1.602*10-19 C (electron charge).

k=1.380*10-23 J/K (Boltzmann constant).

Eg=1.12 eV is the band gap energy.

The nominal diode

$$I_0 = I_{an}\left(\frac{T}{T_n}\right)^3 \exp\left[\frac{qE_g}{ak}\left(\frac{1}{T_n}-\frac{1}{T}\right)\right] \quad (4)$$

$$I_{o,n} = \frac{I_{sc,n}}{\left[\exp\left(\frac{V_{oc,n}}{aV_{t,n}}\right)\right]-1}$$

Where:

Vocn = nominal open-circuit voltage;

Vt,n = nominal thermal voltage of the cell;

Isc,n = short-circuit current at the nominal condition (25oC and 1000W/m2).

A practical photovoltaic panel consists of several switched photovoltaic modules consisting of Ns solar cells connected in series and in parallel. Therefore, (1) with a single PV cell should be replaced with (5) to represent a PV generator. [2],[3].

III. DC-DC CONVERTER

Figure 3 below shows a boost or pulse width modulated (PWM) converter. It consists of a DC input voltage source Vg, a controlled switch S, a diode D, a boost inductor L, a filter capacitor C and a load resistor R.

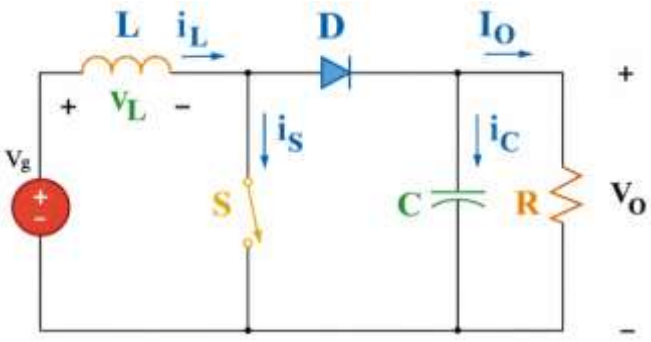

Fig 3: Circuit diagram or boost converter

From the inductor voltage balance equation we have

$$V_g(DT_s) + (V_s - V_0)(1 - D)T_s = 0$$

IV. MPPT

In practical implementations, the photovoltaic (PV) generator is interfaced with a Maximum Power Point Tracking (MPPT) controller to ensure operation at its maximum available power by adjusting the electrical operating point. The MPPT is implemented using a DC DC converter, as illustrated in Fig. 3, which regulates the PV array voltage to operate at the maximum power point voltage Vmp .This voltage regulation is achieved by controlling the converter duty cycle through a pulse-width modulation (PWM) signal applied to the switching device. The PWM signal is generated automatically by an MPPT algorithm. In this work, a Hill Climb (HC) algorithm is employed to control the converter duty cycle. The flowchart of the HC algorithm is shown in Fig. 4 [9]. The algorithm measures the PV array voltage and current to compute the output power and determines the perturbation direction of the duty cycle *D*D. When an increase in power is observed, the perturbation continues in the same direction until the maximum power point (MPP) is reached; otherwise, the direction of perturbation is reversed.

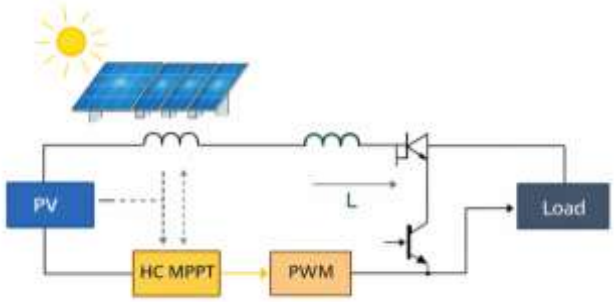

Fig 4 : Block diagram of simulation model

Numerous algorithms have been reported in the literature for maximum power point tracking in photovoltaic systems. Among them, the Perturb and Observe (P&O) and Incremental Conductance (IncCond) methods are adopted in this study due to their fast convergence and low computational complexity.

Perturb and Observe Method (P&O)

The Perturb and Observe (P&O) method is one of the most widely adopted MPPT techniques due to its simplicity and ease of implementation. In this approach, the operating voltage of the photovoltaic (PV) generator is periodically perturbed, and the resulting change in output power is observed. Since the P&O algorithm does not directly measure the exact maximum power point (MPP) voltage, variations in output power are assumed to be caused by the applied voltage perturbation at the PV terminals.A known limitation of the P&O method is the steady-state oscillation around the MPP, which can be mitigated by reducing the perturbation step size. The flowchart of the P&O algorithm is shown in Fig. 3, where changes in the PV terminal voltage determine the adjustment of the converter duty cycle.

The P&O algorithm operates by comparing the instantaneous power P(n+1) with the previous power value P(n) following a voltage or current perturbation. If the perturbation results in an increase in power (dP/dV>0), the operating point is shifted further in the same direction; otherwise, the perturbation direction is reversed. This iterative process continues until the operating point converges to the maximum power point.

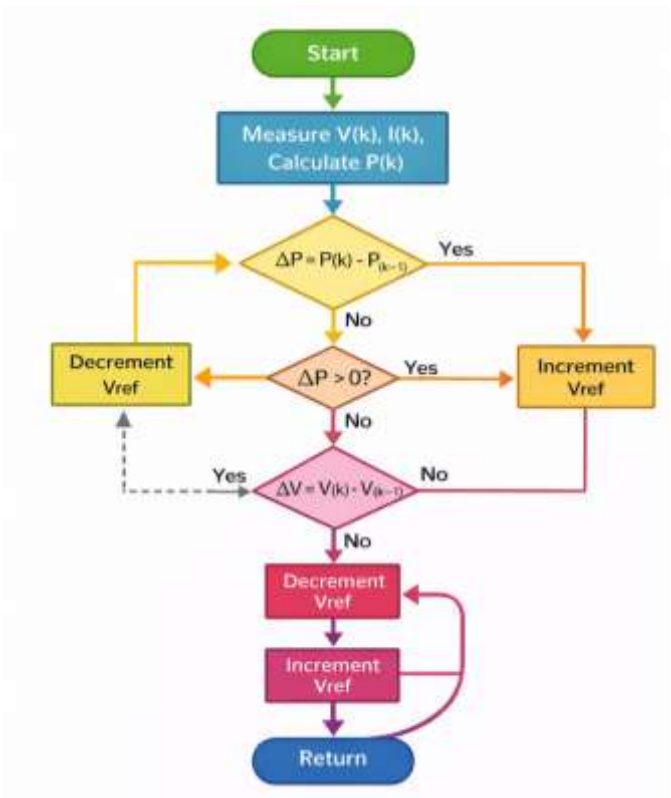

Fig.5 . Flow chart of P&O method

Incremental Conductance method (IncCond)

Conventional MPPT schemes typically employ two cascaded control loops: an outer loop implementing the MPPT algorithm and an inner loop based on a proportional–integral (PI) controller. In such approaches, the Incremental Conductance (IncCond) principle is used to generate an error signal, which becomes zero at the maximum power point (MPP). Since this error is generally nonzero during operation, the inner PI loop is required to drive it toward zero. However, due to the nonlinear characteristics of PV systems and the sensitivity of PI controllers to varying environmental conditions, this structure often results in suboptimal performance.

To overcome these limitations, this work adopts a direct-control Incremental Conductance method, in which the duty cycle of the DC–DC converter is adjusted directly by the MPPT algorithm without using a PI controller. A small allowable error margin of 0.002 is introduced to define the system sensitivity and ensure stable operation. The maximum power condition is defined by (dI/dV= - I/V).

The flowchart of the proposed IncCond-based direct control method is shown in Fig. 4. At each sampling instant, the MPPT algorithm computes the duty cycle, which is applied directly as the reference duty cycle for the subsequent control step.

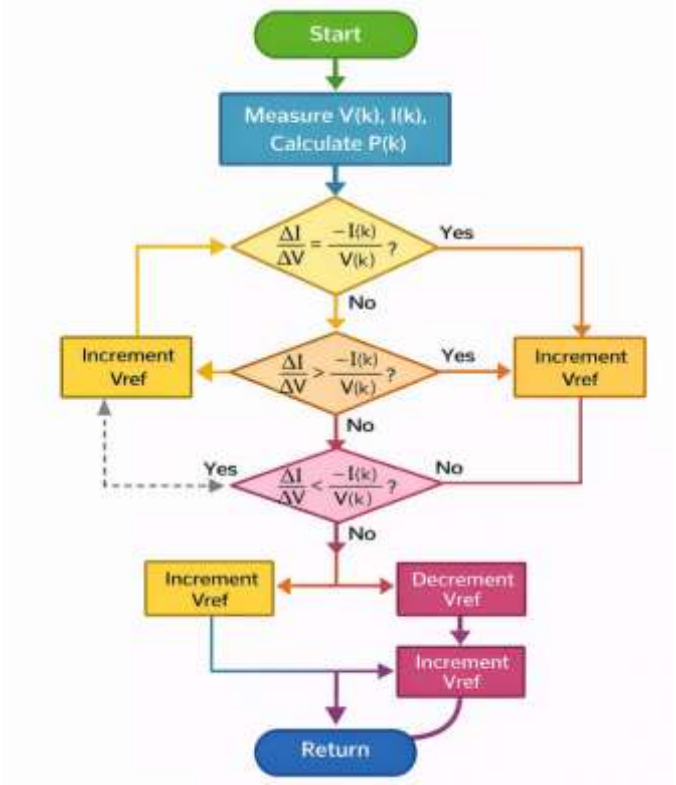

Fig 6 : Flow Chart of Incremental Conductance

V. INVERTER CONTROL

A three-phase three-level neutral-point-clamped (NPC) inverter is employed to enable adjustable-frequency operation with improved power quality and reduced current ripple. A DC-link capacitor stabilizes the input voltage and suppresses harmonic feedback. The voltage source converter regulates the DC-link voltage at 500 V while maintaining unity power factor using a cascaded control structure consisting of an outer DC voltage loop and an inner d-q current control loop for active (I_d)

and reactive (I-q) current regulation with a 100 μs sampling period. The grid-side controller ensures grid synchronization, regulates active and reactive power exchange, maintains a constant DC-link voltage, and enforces acceptable power quality through a fast inner current loop and a slower outer voltage loop, resulting in stable and sinusoidal grid currents suitable for grid-connected operation.

VI. SIMULINK MODEL AND RESULTS

In Simulink various PV array are present and in proposed system Sun Power SPR 305 WHT-D is considered.

Parameters and its values

Parameters	Values
Number of cell per Module	5
Number of parallel string	66
Voc	64.2 V
Vmpp	54.7 V
Impp	5.96 A

In this paper modeling and simulation of a 100 kWp solar PV power plant has been done. MPPT method have been employed and it has been observed that the generation of power increases with increase in irradiance.

In this paper we present the mathematical modeling of PV and its IV characteristics by MATLAB R2020a software. This paper suggests that MPPT algorithm can be enabled with boost converter circuit so as to get better results with PV modules so as to get continuous supply with a PV grid integrated system. The overall controlling input parameter for generating power with PV module is temperature and irradiance and it has been seen that the generated PV power is inversely proportional to the temperature whereas it is directly proportional to the irradiance level measured in w/m.

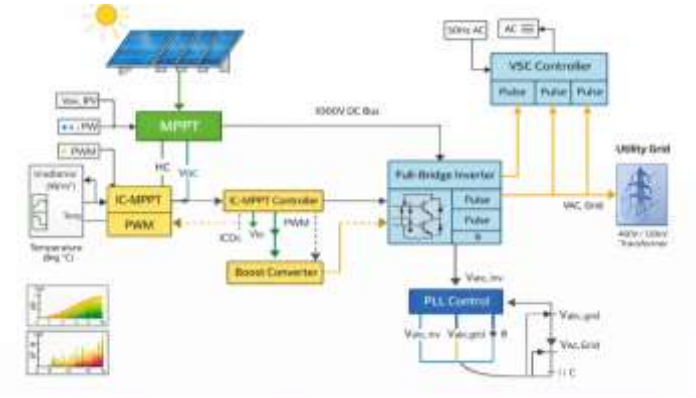

Fig 7 : Simulation Model of Hybrid Microgrid based on MPPT

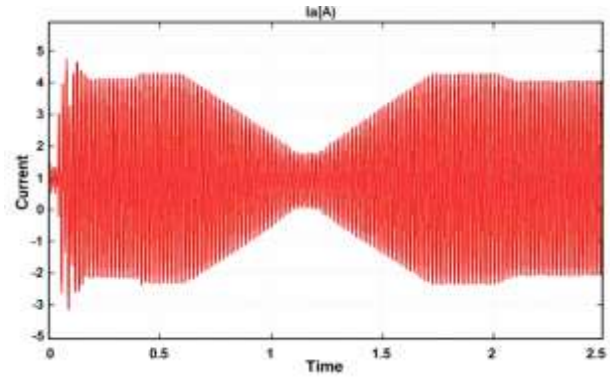

Fig 8: Current At Bus

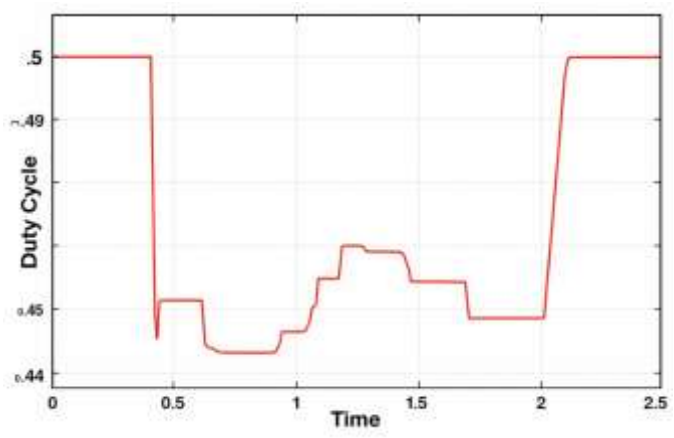

Fig 9: Duty cycle of the boost converter

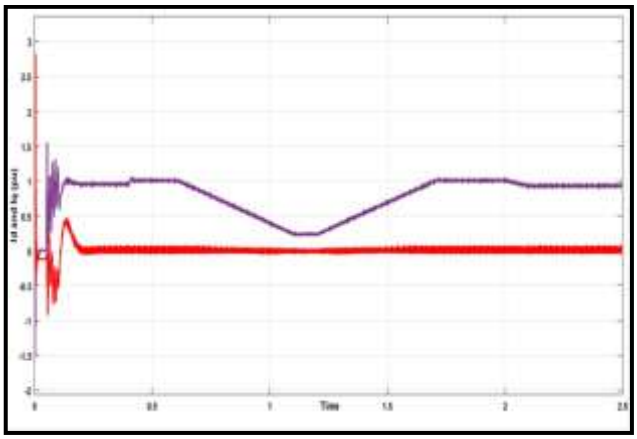

Fig 10: Id and Iq Current in pu

The figure 8 illustrates the phase-A inverter/grid current I_a which remains predominantly sinusoidal, confirming proper grid synchronization and effective current control. Initial oscillations correspond to startup transients, after which the waveform stabilizes. The temporary reduction in current amplitude indicates a decrease in injected power due to variations in operating conditions such as irradiance or DC-link power, while the subsequent recovery demonstrates the ability of the grid-side controller to dynamically regulate active power and maintain stable grid-connected operation.

The figure 9 shows the variation of the DC–DC converter duty cycle with time. Initially, the duty cycle is high, indicating a higher voltage boost to extract maximum power from the PV array during startup. A sudden drop around the early time interval reflects a change in operating conditions, such as reduced irradiance or a shift in the maximum power point (MPP). The subsequent stepwise adjustments demonstrate the MPPT algorithm's operation, where the duty cycle is incrementally increased or decreased to track the new MPP. Finally, the duty cycle stabilizes at a higher value, confirming convergence of the MPPT algorithm and steady-state

operation with optimal power extraction under restored conditions.

After t=2.1s the duty cycle starts increasing and again reaches to its maximum value of .5.

Figure 10 shows the direct and quadrature current per unit values for the designed model. I_D and Iq attains its maximum value of 1.5pu at time t=0.1s.

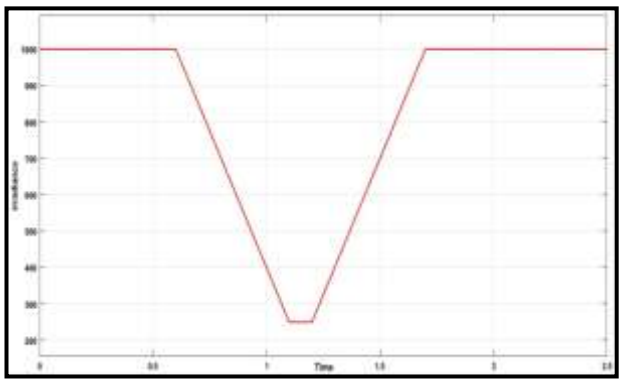

Fig 11: Irradiance of PV Array

Fig. 11 illustrates the solar irradiance profile applied to the PV modules. The irradiance initially remains at its maximum value of 1000 W/m². At t = 0.6 **s**, the irradiance begins to decrease and reaches a minimum level of 250 W/m² at t = 1.1 **s**. After t = 1.2 **s**, the irradiance gradually increases and finally returns to its peak value of 1000 W/m² at t = 1.7 **s**, representing a dynamic variation in solar conditions.

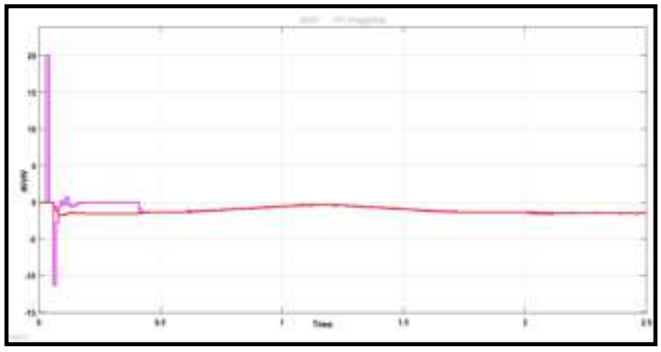

Fig 12: MPPT algorithm di/dv

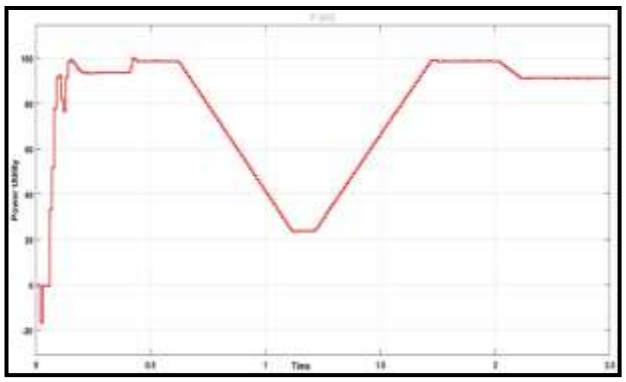

Fig 13: Power Utility

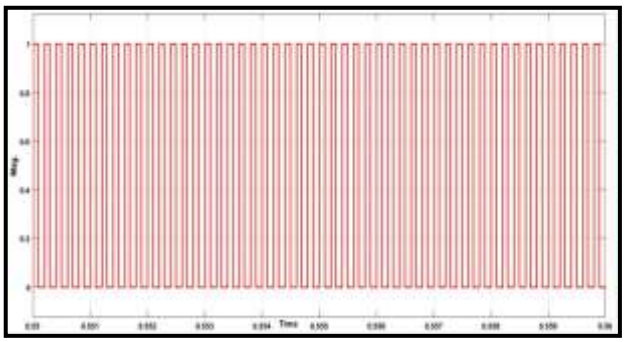

Fig 14: Pulse MPPT

The figure 14 shows the pulse-width modulation (PWM) signal generated by the MPPT controller for the DC–DC converter or inverter switch. The waveform alternates between logic high (1) and logic low (0), indicating the ON–OFF switching of the power semiconductor device at a constant switching frequency. The duty cycle of the PWM signal determines the effective output voltage of the converter and is continuously adjusted by the MPPT algorithm to track the maximum power point. The uniform switching pattern confirms stable controller operation, while any variation in pulse width reflects changes in operating conditions such as irradiance or temperature to ensure optimal power extraction.

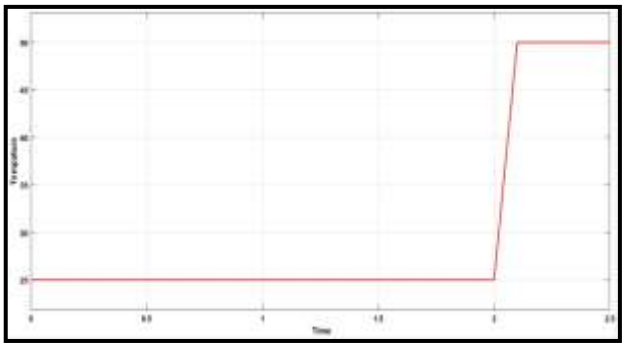

Fig 15: Temperature

Fig 15 shows Initially, the temperature remains constant at 25 °C, representing standard operating conditions. At approximately t = 2 s, a sudden increase in temperature is observed, rising to about 50 °C, which simulates a rapid change in environmental or operating conditions. This step change is useful for evaluating the robustness of the PV system and MPPT controller under thermal disturbances, as increased temperature directly affects

PV voltage, power output, and overall system efficiency.

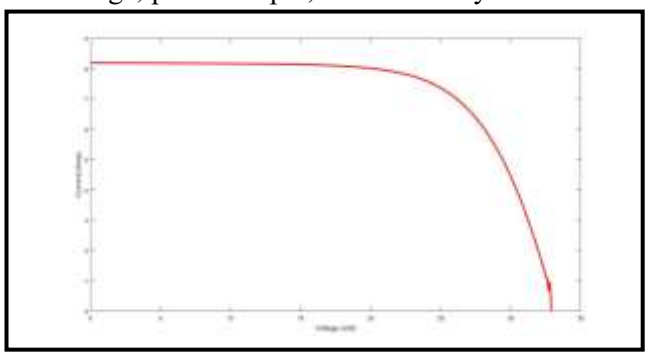

Fig 16: I-V Curve

The maximum power point of a solar cell represents the utilization of a PV modules to its full extent. Here the coordinates for maximum power point current and voltage are [7.9A, 26V]. under a given irradiance and temperature condition. At low voltage levels, the PV current remains nearly constant, indicating operation in the current-source region where the output current is close to the short-circuit current. As the voltage increases, the current starts to decrease gradually and then drops sharply near the knee of the curve, which corresponds to the maximum power point (MPP). Beyond this point, a small increase in voltage causes a significant reduction in current, and the curve approaches the open-circuit voltage where the output current becomes zero. This characteristic highlights the nonlinear behavior of PV modules and emphasizes the importance of MPPT algorithms to ensure operation near the knee region for maximum power extraction.

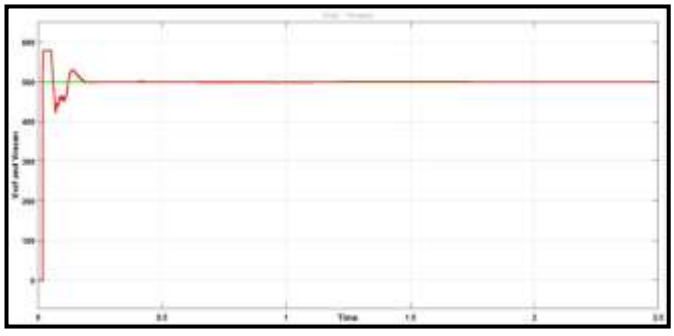

Fig 17: Vref and Vmean

Mean voltage for inverter circuit is shown below in which the reference value is set at 500V whereas the mean value reaches its maximum value of 508V within fraction of seconds from 0.

CONCLUSION

In this work, modeling and simulation of a photovoltaic solar installation of 100 kWp. The 100 kWp system consists of five 20 kW systems connected in parallel. MPPT methods including IncCond were used to run the simulation in MATLAB/Simulink on the 100 kW system. It was observed that, as expected, the generated power increased as the irradiance increased. However, the IncCond method showed a decrease in the duty cycle when the luminance was changed. The slight difference is due to the variation of the PV module parameters available in MATLAB. This modified MPPT algorithm is able to increase the stable and dynamic performance of the PV system. This allows us to extract maximum energy from solar radiation and ensure a stable and efficient power supply. The above results indicated that the proposed MPPT algorithm can be efficient in tracking the maximum amount of radiation and also providing the maximum energy for the PV array. Moreover, this proposed MPPT algorithm gave us maximum power at low cost and less energy loss.

REFERENCES

[1] M. Thakur and S. P. Makhija, “Comparative performance analysis of MPPT algorithms for grid-interconnected photovoltaic systems,” *Int. J. Sci. Res. Eng. Manag.*, vol. 10, no. 1, pp. 1–8, Jan. 2026.

[2] A. Verma, R. Kumar, and P. Singh, “Advanced MPPT techniques for grid-connected PV systems: A review,” *IEEE Access*, vol. 13, pp. 11245–11260, 2025.

[3] S. Padmanaban et al., “Control and integration of grid-connected photovoltaic systems,” *Renew. Sustain. Energy Rev.*, vol. 186, pp. 113–128, 2024.

[4] H. Rezk and A. Fathy, “Optimal MPPT control of photovoltaic systems under dynamic conditions,” *Energy Convers. Manag.*, vol. 285, pp. 116–129, 2023.

[5] Y. Yang, F. Blaabjerg, and H. Wang, “Low-voltage ride-through of grid-connected photovoltaic systems,” *IEEE Trans. Ind. Appl.*, vol. 58, no. 6, pp. 6825–6836, 2022.

[6] M. Abdelrahem, R. Kennel, and J. Rodríguez, “Model predictive control for grid-connected converters,” *IEEE Trans. Power Electron.*, vol. 36, no. 10, pp. 11340–11352, 2021.

[7] T. Esram and P. L. Chapman, "Comparison of photovoltaic array maximum power point tracking techniques," *IEEE Trans. Energy Convers.*, vol. 22, no. 2, pp. 439–449, 2020.

[8] M. Killi and S. Samanta, "Adaptive MPPT techniques for photovoltaic systems," *IET Renew. Power Gener.*, vol. 13, no. 7, pp. 1098–1109, 2019.

[9] A. Safari and S. Mekhilef, "Simulation and hardware implementation of incremental conductance MPPT," *Int. J. Electr. Power Energy Syst.*, vol. 95, pp. 99–109, 2018.

[10] F. Blaabjerg, Z. Chen, and S. B. Kjaer, "Power electronics as efficient interface in dispersed power generation systems," *IEEE Trans. Power Electron.*, vol. 33, no. 7, pp. 5383–5400, 2017.

[11] M. G. Villalva, J. R. Gazoli, and E. R. Filho, "Comprehensive approach to modeling and simulation of photovoltaic arrays," *IEEE Trans. Power Electron.*, vol. 24, no. 5, pp. 1198–1208, 2016.

[12] N. Femia, G. Petrone, G. Spagnuolo, and M. Vitelli, "Optimization of perturb and observe MPPT method," *IEEE Trans. Power Electron.*, vol. 30, no. 11, pp. 6299–6310, 2015.

[13] H. Patel and V. Agarwal, "MATLAB-based modeling to study the effects of partial shading on PV array," *IEEE Trans. Energy Convers.*, vol. 29, no. 2, pp. 302–310, 2014.

[14] J. M. Carrasco et al., "Power-electronic systems for the grid integration of renewable energy sources," *IEEE Trans. Ind. Electron.*, vol. 60, no. 4, pp. 1186–1203, 2013.

[15] A. Yazdani and R. Iravani, *Voltage-Sourced Converters in Power Systems*. Hoboken, NJ, USA: Wiley, 2012.

[16] S. B. Kjaer, J. K. Pedersen, and F. Blaabjerg, "A review of single-phase grid-connected inverters for photovoltaic modules," *IEEE Trans. Ind. Appl.*, vol. 41, no. 5, pp. 1292–1306, 2011.

[17] N. Mohan, T. M. Undeland, and W. P. Robbins, *Power Electronics: Converters, Applications, and Design*, 3rd ed. New York, NY, USA: Wiley, 2010.

[18] J. A. Gow and C. D. Manning, "Development of a photovoltaic array model for use in power-electronics simulation," *IEE Proc. Electr. Power Appl.*, vol. 146, no. 2, pp. 193–200, 2009.

[19] M. A. Elgendy, B. Zahawi, and D. J. Atkinson, "Assessment of perturb and observe MPPT algorithm implementation techniques," *IEEE Trans. Ind. Electron.*, vol. 55, no. 9, pp. 3484–3492, 2008.

[20] H. Sugimoto and S. Sakane, "Maximum power point tracking control of photovoltaic generation systems," *IEEE Trans. Ind. Appl.*, vol. 43, no. 3, pp. 665–672, 2007.